Impurity effect of the Λ particle on the structure of ^{18}F and $^{19}_{\Lambda}$F

Y. Tanimura and K. Hagino
Department of Physics, Tohoku University, Sendai 980-8578, Japan

H. Sagawa
Center for Mathematics and Physics, University of Aizu, Aizu-Wakamatsu, Fukushima 965-8560, Japan and RIKEN Nishina Center, Wako 351-0198, Japan

(Received 27 August 2012; published 23 October 2012)

We perform three-body model calculations for a sd-shell hypernucleus $^{19}_{\Lambda}$F ($^{17}_{\Lambda}$O $+ p + n$) and its core nucleus ^{18}F (^{16}O $+ p + n$), employing a density-dependent contact interaction between the valence proton and neutron. We find that the $B(E2)$ value from the first excited state (with spin and parity of $I^{\pi} = 3^+$) to the ground state ($I^{\pi} = 1^+$) is slightly changed by the addition of a Λ particle, which exhibits the so called shrinkage effect of Λ particle. We also show that the excitation energy of the 3^+ state is reduced in $^{19}_{\Lambda}$F compared to ^{18}F, as is observed in a p-shell nucleus ^{6}Li. We discuss the mechanism of this reduction of the excitation energy, pointing out that it is caused by a different mechanism from that in $^{7}_{\Lambda}$Li.

DOI: 10.1103/PhysRevC.86.044331 PACS number(s): 21.80.+a, 21.60.Cs, 27.20.+n, 23.20.Lv

I. INTRODUCTION

It has been of great interest in hypernuclear physics to investigate how Λ particle affects the core nucleus when it is added to a normal nucleus. A Λ particle may change various nuclear properties, e.g., nuclear size and shape [1–5], cluster structure [6], the neutron drip line [7,8], the fission barrier [9], and the collective excitations [10,11]. Such effects caused by Λ on nuclear properties are referred to as an impurity effect. Because Λ particle can penetrate deeply into a nucleus without the Pauli principle from nucleons, a response of the core nucleus to an addition of a Λ may be essentially different from that to nonstrange probes. That is, Λ particle can be a unique probe of nuclear structure that cannot be investigated by normal reactions.

The low-lying spectra and electromagnetic transitions have been measured systematically in p-shell hypernuclei by high precision γ-ray spectroscopy [12]. The experimental data have indicated a shrinkage of nuclei due to the attraction of Λ. A well-known example is $^{7}_{\Lambda}$Li, for which the electric quadrupole transition probability, $B(E2)$, from the first excited state (3^+) to the ground state (1^+) of ^{6}Li is considerably reduced when a Λ particle is added [13,14]. This reduction of the $B(E2)$ value has been interpreted as a shrinkage of the distance between α and d clusters in ^{6}Li. On the other hand, a change of excitation energy induced by a Λ particle depends on nuclides. If one naively regards a dicluster nucleus as a classical rigid rotor, shrinkage of nuclear size would lead to a reduction of the moment of inertia, increasing the rotational excitation energy. However, ^{6}Li and ^{8}Be show a different behavior from this naive expectation. That is, the spin averaged excitation energy decreases in ^{6}Li [15] while it is almost unchanged in ^{8}Be [16].

Recently, Hagino and Koike [17] have applied a semimicroscopic cluster model to ^{6}Li, $^{7}_{\Lambda}$Li, ^{8}Be, and $^{9}_{\Lambda}$Be to successfully account for the relation between the shrinkage effect and the rotational spectra of the two nuclei simultaneously. They argue that a Gaussian-like potential between two clusters leads to a stability of excitation spectrum against an addition of a Λ particle, even though the intercluster distance is reduced. This explains the stabilization of the spectrum in ^{8}Be. In the case of lithium, one has to consider also the spin-orbit interaction between ^{4}He/$^{5}_{\Lambda}$He and the deuteron cluster. Because of the shrinkage effect of Λ, the overlap between the relative wave function and the spin-orbit potential becomes larger in $^{7}_{\Lambda}$Li than in ^{6}Li. This effect lowers the $3^+ \otimes \Lambda_{s_{1/2}}$ state more than the 3^+ state in ^{6}Li, making the rotational excitation energy in $^{7}_{\Lambda}$Li smaller than in ^{6}Li.

These behaviors of the spectra may be specific to the two-body cluster structure. ^{6}Li and ^{8}Be have in their ground states well-developed α cluster structure. In heavier nuclei, on the other hand, cluster structure appears in their excited states while the ground and low-lying states have a mean-field-like structure. In this respect, it is interesting to investigate the impurity effect on a sd-shell nucleus ^{18}F, in which the mean-field structure and ^{16}O $+ d$ cluster structure may be mixed [20–25]. Notice that the ground and the first excited states of ^{18}F are 1^+ and 3^+, respectively, which are the same as ^{6}Li. We mention that a γ-ray spectroscopy measurement for $^{19}_{\Lambda}$F is planned at J-PARC facility as the first γ-ray experiment for sd-shell hypernuclei [18,19].

In this paper we employ a three-body model of ^{16}O $+ p + n$ for ^{18}F and of $^{17}_{\Lambda}$O $+ p + n$ for $^{19}_{\Lambda}$F and study the structure change of ^{18}F caused by the impurity effect of a Λ particle. This model enables us to describe both mean-field and cluster-like structures of these nuclei. We discuss how Λ particle affects the electric transition probability $B(E2, 3^+ \rightarrow 1^+)$, the density distribution of the valence nucleons, and the excitation energy. Of particular interest is whether the excitation energy increases or decreases due to the Λ particle. We discuss the mechanism of its change in comparison with the lithium nuclei.

The paper is organized as follows. In Sec. II, we introduce the three-body model to describe ^{18}F and $^{19}_{\Lambda}$F. In Sec. III, we present the results and discuss the relation between the shrinkage effect and the energy spectrum. In Sec. IV, we summarize the paper.

II. THE MODEL

A. Hamiltonian

We employ a three-body model to describe the ^{18}F and $^{19}_{\Lambda}$F nuclei. We first describe the model Hamiltonian for the ^{18}F nucleus, assuming the ^{16}O + $p + n$ structure. After removing the center-of-mass motion, it is given by

$$H = \frac{\boldsymbol{p}_p^2}{2m} + \frac{\boldsymbol{p}_n^2}{2m} + V_{pC}(\boldsymbol{r}_p) + V_{nC}(\boldsymbol{r}_n) + V_{pn}(\boldsymbol{r}_p, \boldsymbol{r}_n) + \frac{(\boldsymbol{p}_p + \boldsymbol{p}_n)^2}{2A_C m}, \quad (1)$$

where m is the nucleon mass and A_C is the mass number of the core nucleus. V_{pC} and V_{nC} is the mean field potentials for proton and neutron, respectively, generated by the core nucleus. These are given as

$$V_{nC}(\boldsymbol{r}_n) = V^{(N)}(r_n),\ V_{pC}(\boldsymbol{r}_p) = V^{(N)}(r_p) + V^{(C)}(r_p), \quad (2)$$

where $V^{(N)}$ and $V^{(C)}$ are the nuclear and the Coulomb parts, respectively. In Eq. (1), V_{pn} is the interaction between the two valence nucleons. For simplicity, we neglect in this paper the last term in Eq. (1) since the core ^{16}O is much heavier than nucleons. Then the Hamiltonian reads

$$H = h(p) + h(n) + V_{pn}, \quad (3)$$

where the single-particle Hamiltonians are given as

$$h(p) = \frac{\boldsymbol{p}_p^2}{2m} + V_{pC}(\boldsymbol{r}_p), \quad h(n) = \frac{\boldsymbol{p}_n^2}{2m} + V_{nC}(\boldsymbol{r}_n). \quad (4)$$

In this paper, the nuclear part of the mean-field potential, $V^{(N)}$, is taken to be a spherical Woods-Saxon type

$$V_n(r) = \frac{v_0}{1 + e^{(r-R)/a}} + (\boldsymbol{\ell} \cdot \boldsymbol{s})\frac{1}{r}\frac{d}{dr}\frac{v_{\ell s}}{1 + e^{(r-R)/a}}, \quad (5)$$

where the radius and the diffuseness parameters are set to be $R = 1.27A_C^{1/3}$ fm and $a = 0.67$ fm, respectively, and the strengths v_0 and $v_{\ell s}$ are determined to reproduce the neutron single-particle energies of $2s_{1/2}$ (-3.27 MeV) and $1d_{5/2}$ (-4.14 MeV) orbitals in ^{17}O [26]. The resultant values are $v_0 = -49.21$ MeV and $v_{\ell s} = 21.6$ MeV $\cdot$ fm^2. The Coulomb potential $V^{(C)}$ in the proton mean field potential is generated by a uniformly charged sphere of radius R and charge $Z_C e$, where Z_C is the atomic number of the core nucleus. For the pairing interaction V_{pn} we employ a density-dependent contact interaction, which is widely used in similar three-body calculations for nuclei far from the stability line [27–30]. Since we have to consider both the isotriplet and isosinglet channels in our case of proton and neutron, we consider the pairing interaction V_{pn} given by

$$V_{pn}(\boldsymbol{r}_p, \boldsymbol{r}_n) = \hat{P}_s v_s \delta^{(3)}(\boldsymbol{r}_p - \boldsymbol{r}_n)\left[1 + x_s\left(\frac{1}{1 + e^{(r-R)/a}}\right)^{\alpha_s}\right] + \hat{P}_t v_t \delta^{(3)}(\boldsymbol{r}_p - \boldsymbol{r}_n)\left[1 + x_t\left(\frac{1}{1 + e^{(r-R)/a}}\right)^{\alpha_t}\right], \quad (6)$$

where $\hat{P}_s$ and $\hat{P}_t$ are the projectors onto the spin-singlet and spin-triplet channels, respectively:

$$\hat{P}_s = \tfrac{1}{4} - \tfrac{1}{4}\boldsymbol{\sigma}_p \cdot \boldsymbol{\sigma}_n, \quad \hat{P}_t = \tfrac{3}{4} + \tfrac{1}{4}\boldsymbol{\sigma}_p \cdot \boldsymbol{\sigma}_n. \quad (7)$$

In each channel in Eq. (6), the first term corresponds to the interaction in vacuum while the second term takes into account the medium effect through the density dependence. Here, the core density is assumed to be a Fermi distribution of the same radius and diffuseness as in the mean field, Eq. (5). The strength parameters, v_s and v_t, are determined from the proton-neutron scattering length as [28]

$$v_s = \frac{2\pi^2\hbar^2}{m}\frac{2a_{pn}^{(s)}}{\pi - 2a_{pn}^{(s)}k_{\rm cut}}, \quad (8)$$

$$v_t = \frac{2\pi^2\hbar^2}{m}\frac{2a_{pn}^{(t)}}{\pi - 2a_{pn}^{(t)}k_{\rm cut}}, \quad (9)$$

where $a_{pn}^{(s)} = -23.749$ fm and $a_{pn}^{(t)} = 5.424$ fm [31] are the empirical p-n scattering length of the spin-singlet and spin-triplet channels, respectively, and $k_{\rm cut}$ is the momentum cut-off introduced in treating the delta function. The density-dependent terms have two parameters, x and α, for each channel, which are to be determined so as to reproduce the ground and excited state energies of ^{18}F (see Sec. III).

B. Model space

The Hamiltonian, Eq. (3), is diagonalized in the valence two-particle subspace. The basis is given by a product of proton and neutron single-particle states:

$$h(\tau)\left|\psi_{n\ell jm}^{(\tau)}\right\rangle = \epsilon_{n\ell j}^{(\tau)}\left|\psi_{n\ell jm}^{(\tau)}\right\rangle, \quad \tau = p \text{ or } n, \quad (10)$$

where the single-particle continuum states can be discretized in a large box. Here, n is the principal quantum number, ℓ is the orbital angular momentum, j is the total angular momentum of the single-particle state, and $m = j_z$ is the projection of the total angular momentum j. $\epsilon_{n\ell j}^{(\tau)}$ is the single-particle energy. The wave function for states of the total angular momentum I is expanded as

$$|\Psi_{IM_I}\rangle = \sum_{\alpha\beta} C_{\alpha\beta}^I |\alpha\beta, IM_I\rangle, \quad (11)$$

where $C_{\alpha\beta}^I$ are the expansion coefficients. The basis state $|\alpha\beta, IM_I\rangle$ is given by the product

$$\langle \boldsymbol{r}_p \boldsymbol{r}_n | \alpha\beta, IM_I\rangle = \phi_\alpha^{(p)}(r_p)\phi_\beta^{(n)}(r_n)[\mathscr{Y}_{\ell_\alpha j_\alpha}(\hat{\boldsymbol{r}}_p)\mathscr{Y}_{\ell_\beta j_\beta}(\hat{\boldsymbol{r}}_n)]_{IM_I}, \quad (12)$$

where α is a shorthanded notation for single-particle level $\{n_\alpha, \ell_\alpha, j_\alpha\}$, and similarly for β. $\phi_\alpha^{(\tau)}(r_\tau)$ is the radial part of the wave function $\psi_\alpha^{(\tau)}$ of level α, and $\mathscr{Y}_{\ell jm} = \sum_{m'm''}\langle \ell m' \tfrac{1}{2} m'' | jm\rangle Y_{\ell m'}\chi_{\frac{1}{2}m''}$ is the spherical spinor, $\chi_{\frac{1}{2}m''}$ being the spin wave function of nucleon. $\ell_\alpha + \ell_\beta$ is even (odd) for positive (negative) parity state. Notice that we do not use the isospin formalism, with which the number of the basis states, Eq. (12), can be reduced by explicitly taking the antisymmetrization. Instead, we use the proton-neutron formalism without the antisymmetrization in order to take into account the breaking of the isospin symmetry due to the Coulomb term $V^{(C)}$ in Eq. (2).

As shown in the Appendix A, the matrix elements of the spin-singlet channel in V_{pn} identically vanish for the 1^+ and 3^+ states. Thus, we keep only the spin-triplet channel interaction and determine x_t and α_t from the binding energies of the two states from the three-body threshold. In constructing the basis we effectively take into account the Pauli principle and exclude the single-particle $1s_{1/2}$, $1p_{3/2}$, and $1p_{1/2}$ states, which are already occupied by the core nucleons. The cut-off energy $E_{\rm cut}$ to truncate the model space is related with the momentum cut-off in Eq. (9) by $E_{\rm cut} = \hbar^2 k_{\rm cut}^2/m$. We include only those states satisfying $\epsilon_\alpha^{(p)} + \epsilon_\beta^{(n)} \leqslant E_{\rm cut}$.

C. Addition of a Λ particle

Similar to the ^{18}F nucleus, we also treat $^{19}_{\Lambda}$F as a three-body system composed of $^{17}_{\Lambda}\mathrm{O} + p + n$. We assume that the Λ particle occupies the $1s_{1/2}$ orbital in the core nucleus and provides an additional contribution to the core-nucleon potential,

$$V^{(N)}(r) \to V^{(N)}(r) + V_\Lambda(r). \tag{13}$$

We construct the potential V_Λ by folding the N-Λ interaction $v_{N\Lambda}$ with the density ρ_Λ of the Λ particle:

$$V_\Lambda(r) = \int d^3 r_\Lambda\ \rho_\Lambda(\boldsymbol{r}_\Lambda) v_{N\Lambda}(\boldsymbol{r} - \boldsymbol{r}_\Lambda). \tag{14}$$

We use the central part of a N-Λ interaction by Motoba *et al.* [1]:

$$v_{\Lambda N}(r) = v_\Lambda e^{-r^2/b_v^2}, \tag{15}$$

where $b_v = 1.083$ fm, and we set $v_\Lambda = -20.9$ MeV, which is used in the calculation for ^{6}Li in Ref. [17]. The density $\rho_\Lambda(r)$ is given by that of a harmonic oscillator wave function

$$\rho_\Lambda(r) = \left(\pi b_\Lambda^2\right)^{-3/2} e^{-r^2/b_\Lambda^2}, \tag{16}$$

where we take $b_\Lambda = \sqrt{(A_C/4)^{1/3}(A_C m + m_\Lambda)/A_C m_\Lambda} \cdot 1.358$ fm, following Refs. [1] and [17].

The total wave function for the $^{19}_{\Lambda}$F nucleus is given by

$$\left|\Psi_{JM}^{\rm tot}\right\rangle = [|\Phi_{I_c}\rangle|\Psi_I\rangle]^{(JM)}, \tag{17}$$

where J is the total angular momentum of the $^{19}_{\Lambda}$F nucleus, $|\Phi_{I_c}\rangle$ is the wave function for the core nucleus, $^{17}_{\Lambda}$O, in the ground state with the spin-parity of $I_c^\pi = 1/2^+$, and $|\Psi_I\rangle$ is the wave function for the valence nucleons with the angular momentum I given by Eq. (11). As we use the spin-independent N-Λ interaction in Eq. (15), the doublet states with $J = I \pm 1/2$ are degenerate in energy.

D. *E*2 transition and the polarization charge

We calculate the reduced electric transition probability, $B(E2, 3^+ \to 1^+)$, as a measure of nuclear size. In our three-body model, the $E2$ transition operator $Q_{2\mu}$ is given by

$$\begin{aligned}
Q_{2\mu} = {} & \frac{(Z_C e + e^{(n)})m^2 + e^{(p)}(M_C + m)^2}{(M_C + 2m)^2} r_p^2 Y_{2\mu}(\hat{\boldsymbol{r}}_p) \\
& + \frac{(Z_C e + e^{(p)})m^2 + e^{(n)}(M_C + m)^2}{(M_C + 2m)^2} r_n^2 Y_{2\mu}(\hat{\boldsymbol{r}}_n) \\
& + 2\frac{Z_C e m^2 - (e^{(p)} + e^{(n)})m(M_C + m)}{(M_C + 2m)^2} \\
& \times \sqrt{\frac{10\pi}{3}} r_p r_n [Y_1(\hat{\boldsymbol{r}}_p) Y_1(\hat{\boldsymbol{r}}_n)]^{(2\mu)}.
\end{aligned} \tag{18}$$

Here, M_C is the mass of the core nucleus, that is, $A_C m$ for ^{18}F and $A_C m + m_\Lambda$ for $^{19}_{\Lambda}$F, where m_Λ is the mass of Λ particle. In Eq. (18), the effective charges of proton and neutron are given as

$$e^{(p)} = e + e_{\rm pol}^{(p)}, \quad e^{(n)} = e_{\rm pol}^{(n)}, \tag{19}$$

respectively. Here we have introduced the polarization charge $e_{\rm pol}^{(\tau)}$ to protons and neutrons to take into account the core polarization effect (in principle one may also consider the polarization charge for the Λ particle, but for simplicity we neglect it in this paper). Their values are determined so as to reproduce the measured $B(E2)$ values of $1/2^+ \to 5/2^+$ transitions in ^{17}F ($64.9 \pm 1.3\ e^2$fm^4) and ^{17}O ($6.21 \pm 0.08\ e^2$fm^4) [32]. In our model we calculate them as single-particle transitions in ^{17}F ($^{16}\mathrm{O} + p$) and in ^{17}O ($^{16}\mathrm{O} + n$). The resultant values are $e_{\rm pol}^{(p)} = 0.098e$ and $e_{\rm pol}^{(n)} = 0.40e$, which are close to the values given in Ref. [33].

The $B(E2)$ value from the 3^+ state to the 1^+ ground state is then computed as,

$$B(E2, 3^+ \to 1^+) = \tfrac{1}{7}\ |\langle \Psi_{J=1} \| Q_2 \| \Psi_{J=3} \rangle|^2, \tag{20}$$

where $\langle \Psi_{J=1} \| Q_2 \| \Psi_{J=3} \rangle$ is the reduced matrix element. We will compare this with the corresponding value for the $^{19}_{\Lambda}$F nucleus, that is,

$$\begin{aligned}
& \tfrac{1}{7}\ |\langle \Psi_{I=1} \| Q_2 \| \Psi_{I=3} \rangle|^2 \\
& = \tfrac{1}{8} \left|\left\langle \left[\Phi_{I_c} \Psi_{I=1}\right]^{J=3/2} \| Q_2 \| \left[\Phi_{I_c} \Psi_{I=3}\right]^{J=7/2} \right\rangle\right|^2, \qquad (21) \\
& = \tfrac{1}{6} \left|\left\langle \left[\Phi_{I_c} \Psi_{I=1}\right]^{J=3/2} \| Q_2 \| \left[\Phi_{I_c} \Psi_{I=3}\right]^{J=5/2} \right\rangle\right|^2 \\
& \quad + \tfrac{1}{6} \left|\left\langle \left[\Phi_{I_c} \Psi_{I=1}\right]^{J=1/2} \| Q_2 \| \left[\Phi_{I_c} \Psi_{I=3}\right]^{J=5/2} \right\rangle\right|^2, \qquad (22)
\end{aligned}$$

which is valid in the weak coupling limit [5,6,13,14] (see Appendix B for the derivation).

III. RESULTS AND DISCUSSION

We now numerically solve the three-body Hamiltonians. Because ^{18}F is a well-bound nucleus so that the cut-off does not have to be high, we use $E_{\rm cut} = 10$ MeV. We have confirmed that the result does not drastically change, even if we use a larger value of the cut-off energy, $E_{\rm cut} = 50$ MeV. Especially the ratio (≈0.96) of the $B(E2)$ value for $^{19}_{\Lambda}$F to that for ^{18}F is quite stable against the cut-off energy. We fit the parameters in the proton-neutron pairing interaction, x_t and α_t, to the energy of the ground state (−9.75 MeV) and that of the first excited state (−8.81 MeV) of ^{18}F. Their values are $x_t = -1.239$ and

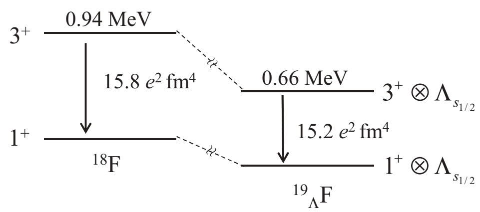

FIG. 1. The level scheme and the $B(E2)$ values for the ^{18}F and $^{19}_{\Lambda}$F nuclei. For the $^{19}_{\Lambda}$F nucleus, a sum of the $B(E2)$ values for the $[3^+ \otimes \Lambda_{s_{1/2}}]^{J=5/2} \to [1^+ \otimes \Lambda_{s_{1/2}}]^{J=3/2}$ and the $[3^+ \otimes \Lambda_{s_{1/2}}]^{J=5/2} \to [1^+ \otimes \Lambda_{s_{1/2}}]^{J=1/2}$ transitions is shown, which corresponds to the $B(E2)$ value from the 3^+ to the 1^+ states in ^{18}F (see the text for details). The excitation energies are shown on the top of each state. The measured $B(E2)$ value for ^{18}F is $16 \pm 0.6\, e^2$fm^4 [26].

$\alpha_t = 0.6628$ for $E_{\mathrm{cut}} = 10$ MeV. We use the box size of $R_{\mathrm{box}} = 30$ fm.

The obtained level schemes of ^{18}F and $^{19}_{\Lambda}$F as well as the $B(E2)$ values are shown in Fig. 1. The $B(E2, 3^+ \to 1^+)$ value is reduced, which indicates that the nucleus shrinks by the attraction of Λ. In fact, as shown in Table I, the root mean square (rms) distance between the core and the center-of-mass of the two valence nucleons, $\langle r^2_{C-pn}\rangle^{1/2}$, and that between the proton and the neutron, $\langle r^2_{p-n}\rangle^{1/2}$, slightly decrease by adding Λ.

To make the shrinkage effect more visible, we next show the two-particle density. The two-particle density $\rho_2(\mathbf{r}_p, \mathbf{r}_n)$ is defined by

$$\rho_2(\boldsymbol{r}_p, \boldsymbol{r}_n) = \sum_{\sigma_p \sigma_n} \langle \boldsymbol{r}_p \sigma_p, \boldsymbol{r}_n \sigma_n | \Psi_{IM} \rangle \langle \Psi_{IM} | \boldsymbol{r}_p \sigma_p, \boldsymbol{r}_n \sigma_n \rangle, \quad (23)$$

where σ_p and σ_n is the spin coordinates of proton and neutron, respectively. Setting $\hat{\boldsymbol{r}}_p = 0$, the density is normalized as

$$\int_0^\infty 4\pi r_p^2 dr_p \int_0^\infty r_n^2 dr_n \times \int_0^\pi 2\pi \sin\theta_{pn} d\theta_{pn}\, \rho_2(r_p, r_n, \theta_{pn}) = 1, \quad (24)$$

where $\theta_{pn} = \theta_n$ is the angle between proton and neutron. In Fig. 2 we show the ground-state density distributions of ^{18}F (the upper panel) and $^{19}_{\Lambda}$F (the lower panel) as a function of $r = r_p = r_n$ and θ_{pn}. They are weighted by a factor of

TABLE I. The core-pn and p-n rms distances, the opening angle between the valence nucleons, and the probability for the spin-triplet component for the ground and the first excited states of ^{18}F and $^{19}_{\Lambda}$F.

		$\langle r^2_{C-pn}\rangle^{1/2}$ (fm)	$\langle r^2_{p-n}\rangle^{1/2}$ (fm)	θ_{pn} (deg)	$P(S=1)$ (%)
1^+	^{18}F	2.72	5.38	89.6	58.6
$1^+ \otimes \Lambda_{s_{1/2}}$	$^{19}_{\Lambda}$F	2.70	5.33	89.5	58.4
3^+	^{18}F	2.71	5.42	84.9	85.0
$3^+ \otimes \Lambda_{s_{1/2}}$	$^{19}_{\Lambda}$F	2.68	5.35	84.7	85.9

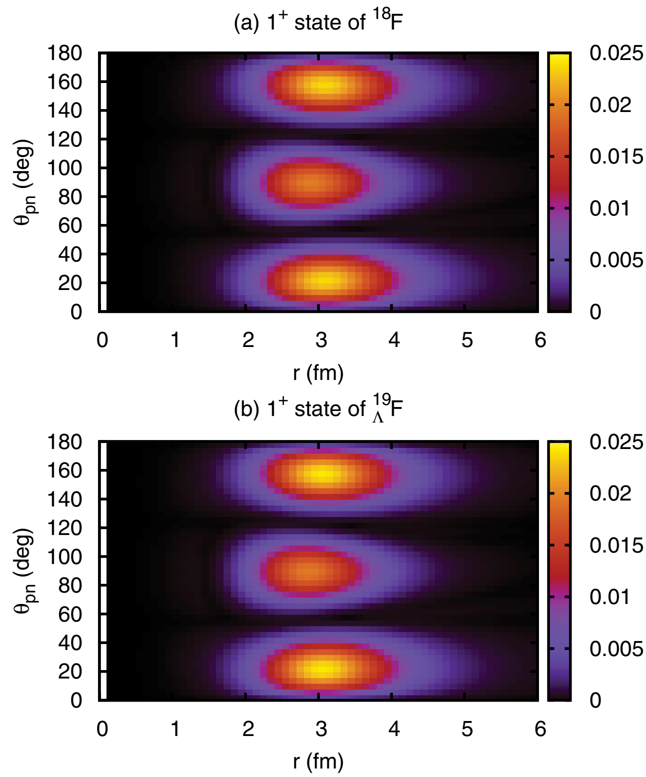

FIG. 2. (Color online) The two-particle densities of the ground state of (a) ^{18}F and (b) $^{19}_{\Lambda}$F as a function of $r_p = r_n \equiv r$ and the opening angle between the proton and the neutron, θ_{pn}. Those densities are multiplied by a weight factor of $8\pi^2 r^4 \sin\theta_{\mathrm{pn}}$ and are given in units of fm^{-3}.

$8\pi^2 r^4 \sin\theta_{pn}$. The distribution slightly moves inward after adding a Λ particle. To see the change clearer, we show in Fig. 3 the difference of the two-particle densities, $\rho_2(^{19}_{\Lambda}\mathrm{F}) - \rho_2(^{18}\mathrm{F})$, for both the 1^+ and the 3^+ states. One can now clearly see that the density distribution is pulled toward the origin by additional attraction caused by the Λ particle both for the 1^+ and the 3^+ states.

Let us next discuss the change in excitation energy. As shown in Fig. 1, it is decreased by addition of Λ, similar to ^{6}Li and $^7_{\Lambda}$Li. In order to clarify the mechanism of this reduction we estimate the energy gain of each valence configuration, treating $V_\Lambda(r_p) + V_\Lambda(r_n) = \Delta V$ by the first-order perturbation theory:

$$\begin{aligned} \Delta E_I &= \left\langle \Psi^{(IM_I)}_{^{18}\mathrm{F}} \middle| \Delta V \middle| \Psi^{(IM_I)}_{^{18}\mathrm{F}} \right\rangle \\ &= \sum_{j_\alpha \ell_\alpha} \sum_{j_\beta \ell_\beta} \sum_{n_\alpha n_{\alpha'}} \sum_{n_\beta n_{\beta'}} C^{I*}_{n_{\alpha'}\ell_\alpha j_\alpha, n_{\beta'}\ell_\beta j_\beta} C^{I}_{n_\alpha \ell_\alpha j_\alpha, n_\beta \ell_\beta j_\beta} \\ &\quad \times \left[\delta_{n_{\beta'} n_\beta} \int_0^\infty r_p^2 dr_p\, \phi^{(p)}_{n_{\alpha'}\ell_\alpha j_\alpha}(r_p)^* V_\Lambda(r_p) \phi^{(p)}_{n_\alpha \ell_\alpha j_\alpha}(r_p) \right. \\ &\quad \left. + \delta_{n_{\alpha'} n_\alpha} \int_0^\infty r_n^2 dr_n\, \phi^{(n)}_{n_{\beta'}\ell_\beta j_\beta}(r_n)^* V_\Lambda(r_n) \phi^{(n)}_{n_\beta \ell_\beta j_\beta}(r_n) \right] \\ &\equiv \sum_{j_\alpha \ell_\alpha j_\beta \ell_\beta} \Delta\epsilon^{(I)}_{j_\alpha \ell_\alpha j_\beta \ell_\beta}, \end{aligned} \quad (25)$$

where $\Delta\epsilon^{(I)}_{j_\alpha \ell_\alpha j_\beta \ell_\beta}$ is the contribution of each configuration to the total approximate energy change ΔE_I. We show in the

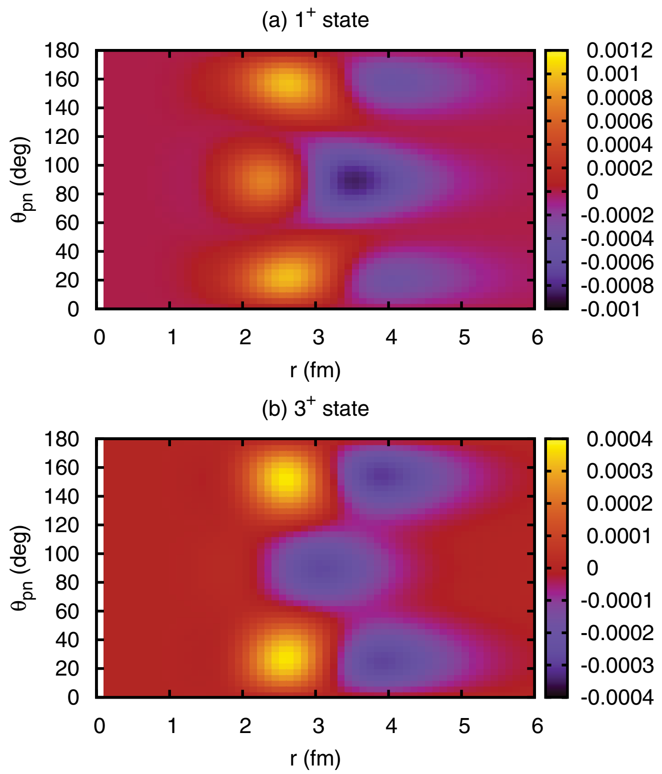

FIG. 3. (Color online) The difference of the density distribution in units of fm^{-3} between $^{19}_{\Lambda}$F and ^{18}F for (a) the 1^+ state and (b) the 3^+ state.

first and the second columns in Table II dominant valence configurations and their occupation probabilities. In the third and the fourth columns of Table II are the energy gains of each configuration $\Delta\epsilon$ and $\Delta\epsilon/P$, respectively, where P is the occupation probability in the ^{18}F nucleus of the corresponding configuration. Notice that $\Delta\epsilon/P$ is the largest for the $s \otimes s$ configuration, and the second largest for the $s \otimes d$ and $d \otimes s$, because s-wave states have more overlap with the Λ occupying the $1s_{1/2}$ orbital. In the ground state of ^{18}F, both proton and neutron occupy s-wave states with a probability of 11.63%, while in the excited 3^+ state one of the two valence nucleons occupies an s-wave state with a probability of 55.71%. Thus, the 3^+ state has much more s-wave component than the 1^+ state. Therefore, the valence nucleons in the 3^+ state have more overlap with the Λ particle and gain more binding compared to the ground state. In fact, as one can see in Table II, the probabilities of the configurations with s wave grow up by adding Λ.

TABLE II. Dominant configurations and their occupation probabilities for the 1^+ and 3^+ states of ^{18}F and $^{19}_{\Lambda}$F. The energy gains of each configuration estimated by the first-order perturbation theory are also shown in the third and fourth columns, where P is the occupation probability in the ^{18}F nucleus.

Configuration	Occupation probability ^{18}F	Occupation probability $^{19}_{\Lambda}$F	$\Delta\epsilon$ (MeV)	$\Delta\epsilon/P$ (MeV)
		1^+ state		
$\pi_{d_{5/2}} \otimes \nu_{d_{5/2}}$	53.69%	54.29%	−0.38	−0.71
$\pi_{d_{3/2}} \otimes \nu_{d_{5/2}}$	15.85%	15.02%	−0.10	−0.63
$\pi_{d_{5/2}} \otimes \nu_{d_{3/2}}$	15.41%	14.57%	−0.10	−0.65
$\pi_{s_{1/2}} \otimes \nu_{s_{1/2}}$	11.63%	12.76%	−0.13	−1.12
		3^+ state		
$\pi_{d_{5/2}} \otimes \nu_{d_{5/2}}$	38.30%	35.98%	−0.27	−0.70
$\pi_{s_{1/2}} \otimes \nu_{d_{5/2}}$	28.30%	29.64%	−0.26	−0.92
$\pi_{d_{5/2}} \otimes \nu_{s_{1/2}}$	27.41%	28.68%	−0.26	−0.95

We have repeated the same calculations by turning off the core-nucleon spin-orbit interaction in Eq. (5), which is the origin of the core-deuteron spin-orbit interaction. We have confirmed that the excitation energy still decreases without the spin-orbit interaction. We have also carried out calculations for the ground (0^+) and the first excited (2^+) levels in ^{18}O and $^{19}_{\Lambda}$O with only the spin-singlet (iso-triplet) channel interaction. In this case, even though the spin-orbit interaction between the core and two neutrons is absent, the excitation energy still decreases by adding a Λ particle. Therefore, we find that the mechanism of the reduction of the excitation energy in ^{18}F is indeed different from the case of lithium, where the LS interaction between the core and deuteron plays an important role in the latter.

IV. SUMMARY

We have calculated the energies of the lowest two levels and $E2$ transitions of ^{18}F and $^{19}_{\Lambda}$F using a simple three-body model. It is found that $B(E2, 3^+ \rightarrow 1^+)$ is slightly changed, as is expected from the shrinkage effect of Λ. We have indeed seen that the distance between the valence two nucleons and the ^{16}O core decreases after adding a Λ particle. We also found that excitation energy of the 3^+ state is decreased. We observed that the 3^+ state has much more s-wave component than the ground state and thus gains more binding coupled with the Λ occupying $1s_{1/2}$ orbital. This leads to a conclusion that the excitation energy of the first-core excited state $3^+ \otimes \Lambda_{s_{1/2}}$ of $^{19}_{\Lambda}$F becomes smaller than the corresponding excitation in ^{18}F. We have pointed out that the mechanism of this reduction is different from that of ^{6}Li and $^7_{\Lambda}$Li, where the core-deuteron spin-orbit interaction plays an important role [17]. This may suggest that the information on the wave function of a core nucleus can be studied using the spectroscopy of Λ hypernuclei.

In this paper, we used a spin-independent N-Λ interaction. To be more realistic and quantitative, it is an interesting future work to employ a spin-dependent N-Λ interaction and explicitly take into account the core excitation. It may also be important to explicitly take into account the tensor correlation between the valence proton and neutron.

ACKNOWLEDGMENTS

We thank T. Koike, T. Oishi, and H. Tamura for useful discussions. The work of Y.T. was supported by the Japan Society for the Promotion of Science for Young Scientists. This work was also supported by the JSPS via the Grant-in-Aid program under the program number 24·3429 and the

Japanese Ministry of Education, Culture, Sports, Science and Technology by Grant-in-Aid for Scientific Research under the program number (C) 22540262.

APPENDIX A: MATRIX ELEMENTS OF V_{pn}

In this appendix we explicitly give an expression for the matrix elements of the proton-neutron pairing interaction V_{pn} given by Eq. (6). They read

$$\begin{aligned}\langle\alpha'\beta', IM|V_{pn}|\alpha\beta, IM\rangle &= \langle\alpha'\beta', IM|[\hat{P}_s\delta^{(3)}(\boldsymbol{r}_p-\boldsymbol{r}_n)g_s(r_p)\\ &\quad+\hat{P}_t\delta^{(3)}(\boldsymbol{r}_p-\boldsymbol{r}_n)g_t(r_p)]|\alpha\beta, IM\rangle,\end{aligned}\tag{A1}$$

where we have defined

$$g_s(r) = v_s\left[1+x_s\left(\frac{1}{1+e^{(r-R)/a}}\right)^{\alpha_s}\right],\tag{A2}$$

and similarly for $g_t(r)$. By rewriting the basis into the LS-coupling scheme one obtains

(the singlet term)

$$\begin{aligned}&= \frac{(-)^{\ell_\alpha+j_\beta-\ell_{\alpha'}-j_{\beta'}}}{8\pi}\hat{j}_\alpha\hat{j}_{\alpha'}\hat{j}_\beta\hat{j}_{\beta'}\hat{\ell}_\alpha\hat{\ell}_{\alpha'}\hat{\ell}_\beta\hat{\ell}_{\beta'}\begin{Bmatrix} j_\alpha & j_\beta & I\\ \ell_\beta & \ell_\alpha & \frac{1}{2}\end{Bmatrix}\\ &\times\begin{Bmatrix} j_{\alpha'} & j_{\beta'} & I\\ \ell_{\beta'} & \ell_{\alpha'} & \frac{1}{2}\end{Bmatrix}\begin{pmatrix}\ell_\alpha & \ell_\beta & I\\ 0 & 0 & 0\end{pmatrix}\begin{pmatrix}\ell_{\alpha'} & \ell_{\beta'} & I\\ 0 & 0 & 0\end{pmatrix}\\ &\times\int_0^\infty r^2dr\,\phi_{\alpha'}^{(p)}(r)^*\phi_{\beta'}^{(n)}(r)^*\phi_\alpha^{(p)}(r)\phi_\beta^{(n)}(r)g_s(r),\end{aligned}\tag{A3}$$

and

(the triplet term)

$$\begin{aligned}&= \frac{3}{4\pi}\hat{j}_\alpha\hat{j}_{\alpha'}\hat{j}_\beta\hat{j}_{\beta'}\hat{\ell}_\alpha\hat{\ell}_{\alpha'}\hat{\ell}_\beta\hat{\ell}_{\beta'}\sum_L\hat{L}^2\begin{Bmatrix}\ell_\alpha & \ell_\beta & L\\ \frac{1}{2} & \frac{1}{2} & 1\\ j_\alpha & j_\beta & I\end{Bmatrix}\\ &\times\begin{Bmatrix}\ell_{\alpha'} & \ell_{\beta'} & L\\ \frac{1}{2} & \frac{1}{2} & 1\\ j_{\alpha'} & j_{\beta'} & I\end{Bmatrix}\begin{pmatrix}\ell_\alpha & \ell_\beta & L\\ 0 & 0 & 0\end{pmatrix}\begin{pmatrix}\ell_{\alpha'} & \ell_{\beta'} & L\\ 0 & 0 & 0\end{pmatrix}\\ &\times\int_0^\infty r^2dr\,\phi_{\alpha'}^{(p)}(r)^*\phi_{\beta'}^{(n)}(r)^*\phi_\alpha^{(p)}(r)\phi_\beta^{(n)}(r)g_t(r),\end{aligned}\tag{A4}$$

where $\hat{j}=\sqrt{2j+1}$. From these equations, it is apparent that for odd (even) I and even (odd) parity states, such as 1^+ and 3^+, the singlet term always vanishes because

$$\begin{pmatrix}\ell_\alpha & \ell_\beta & I\\ 0 & 0 & 0\end{pmatrix}=0,\tag{A5}$$

for $\ell_\alpha+\ell_\beta+I=$ odd.

APPENDIX B: EXTRACTION OF THE CORE TRANSITION FROM $B(E2)$ VALUES OF A HYPERNUCLEUS

We consider a hypernucleus with a Λ particle weakly coupled to a core nucleus. In the weak coupling approximation, the wave function for the hypernucleus with angular momentum J and its z-component M is given by

$$\begin{aligned}|JM\rangle &= [|I\rangle\otimes|j_\Lambda\rangle]^{(JM)}\\ &= \sum_{M_I,m_\Lambda}\langle IM_I j_\Lambda m_\Lambda|JM\rangle|IM_I\rangle|j_\Lambda m_\Lambda\rangle,\end{aligned}\tag{B1}$$

where $|IM_I\rangle$ and $|j_\Lambda m_\Lambda\rangle$ are the wave functions for the core nucleus and the Λ particle, respectively. Suppose that the operator $\hat{T}_{\lambda\mu}$ for electromagnetic transitions is independent of the Λ particle. Then, the square of the reduced matrix element of $\hat{T}_{\lambda\mu}$ between two hypernuclear states reads [see Eq. (7.1.7) in Ref. [34] as well as Eq. (6-86) in Ref. [35]],

$$\begin{aligned}|\langle J_f\|T_\lambda\|J_i\rangle|^2 &= (2J_i+1)(2J_f+1)\begin{Bmatrix} I_f & J_f & j_\Lambda\\ J_i & I_i & \lambda\end{Bmatrix}^2\\ &\quad\times\langle I_f\|T_\lambda\|I_i\rangle^2.\end{aligned}\tag{B2}$$

Notice the relation [see Eq. (6.2.9) in Ref. [34]],

$$\sum_{J_f}(2J_f+1)\begin{Bmatrix} I_f & J_f & j_\Lambda\\ J_i & I_i & \lambda\end{Bmatrix}^2=\frac{1}{2I_i+1}.\tag{B3}$$

This yields

$$\begin{aligned}\sum_{J_f}B(E\lambda;J_i\to J_f) &= \sum_{J_f}\frac{1}{2J_i+1}|\langle J_f\|T_\lambda\|J_i\rangle|^2\\ &= \frac{1}{2I_i+1}\langle I_f\|T_\lambda\|I_i\rangle^2,\end{aligned}\tag{B4}$$

which is nothing but the $B(E\lambda)$ value of the core nucleus from the state I_i to the state I_f. This proves Eqs. (21) and (22) in Sec. II for the specific case of $I_i=3$ and $I_f=1$.

[1] T. Motoba, H. Bandō, and K. Ikeda, Prog. Theor. Phys. **70**, 189 (1983).
[2] Myaing Thi Win, K. Hagino, and T. Koike, Phys. Rev. C **83**, 014301 (2011).
[3] Bing-Nan Lu, En-Guang Zhao, and Shan-Gui Zhou, Phys. Rev. C **84**, 014328 (2011).
[4] M. Isaka, M. Kimura, A. Doté, and A. Ohnishi, Phys. Rev. C **83**, 044323 (2011).
[5] Masahiro Isaka, Hiroaki Homma, Masaaki Kimura, Akinobu Doté, and Akira Ohnishi, Phys. Rev. C **85**, 034303 (2012).
[6] Masahiro Isaka, Masaaki Kimura, Akinobu Doté, and Akira Ohnishi, Phys. Rev. C **83**, 054304 (2011).
[7] D. Vretenar, W. Poschl, G. A. Lalazissis, and P. Ring, Phys. Rev. C **57**, 1060(R) (1998).
[8] X.-R. Zhou, A. Polls, H.-J. Schulze, and I. Vidana, Phys. Rev. C **78**, 054306 (2008).
[9] F. Minato, S. Chiba, and K. Hagino, Nucl. Phys. A **831**, 150 (2009); F. Minato and S. Chiba, *ibid.* **856**, 55 (2011).
[10] J. M. Yao, Z. P. Li, K. Hagino, M. Thi Win, Y. Zhang, and J. Meng, Nucl. Phys. A **868**, 12 (2011).
[11] F. Minato and K. Hagino, Phys. Rev. C **85**, 024316 (2012).
[12] O. Hashimoto and H. Tamura, Prog. Part. Nucl. Phys. **57**, 564 (2006), and the references therein.
[13] K. Tanida *et al.*, Phys. Rev. Lett. **86**, 1982 (2001).
[14] E. Hiyama, M. Kamimura, K. Miyazaki, and T. Motoba, Phys. Rev. C **59**, 2351 (1999).
[15] M. Ukai *et al.*, Phys. Rev. C **73**, 012501(R) (2006).
[16] H. Akikawa *et al.*, Phys. Rev. Lett. **88**, 082501 (2002).

[17] K. Hagino and T. Koike, Phys. Rev. C **84**, 064325 (2011).
[18] H. Tamura *et al.*, J-PARC 50 GeV PS proposal E13 (2006), [http://j-parc/NuclPart/pac_0606/pdf/p13-Tamura.pdf].
[19] T. Koike, in *Proceedings of Sendai International Symposium on Strangeness in Nuclear and Hadronic System (SENDAI08)*, edited by K. Maeda *et al.* (World Scientific, Singapore, 2010), p. 213.
[20] T. Sakuda, S. Nagata, and F. Nemoto, Prog. Theor. Phys. **56**, 1126 (1976).
[21] M. LeMere, Y. C. Tang, and D. R. Thompson, Phys. Rev. C **14**, 1715 (1976).
[22] T. Inoue, T. Seve, K. K. Huang, and A. Arima, Nucl. Phys. A **99**, 305 (1967).
[23] B. Buck, A. C. Merchant, and N. Rowley, Nucl. Phys. A **327**, 29 (1979).
[24] B. Buck, H. Friedrich, and A. A. Pilt, Nucl. Phys. A **290**, 205 (1977).
[25] A. C. Merchant, J. Phys. G **9**, 1169 (1983).
[26] D. R. Tilley, H. R. Weller, and C. M. Cheves, Nucl. Phys. A **564**, 1 (1993).
[27] G. F. Bertsch and H. Esbensen, Ann. Phys. (NY) **209**, 327 (1991).
[28] H. Esbensen, G. F. Bertsch, and K. Hencken, Phys. Rev. C **56**, 3054 (1997).
[29] K. Hagino, H. Sagawa, J. Carbonell, and P. Schuck, Phys. Rev. Lett. **99**, 022506 (2007).
[30] T. Oishi, K. Hagino, and H. Sagawa, Phys. Rev. C **82**, 024315 (2010).
[31] L. Koester and W. Nistler, Z. Phys. A **272**, 189 (1975).
[32] F. Ajzenberg-Selove, Nucl. Phys. A **392**, 1 (1983).
[33] Y. Suzuki, H. Matsumura, and B. Abu-Ibrahim, Phys. Rev. C **70**, 051302(R) (2004).
[34] A. R. Edmonds, *Angular Momentum in Quantum Mechanics* (Princeton University Press, Princeton, New Jersey, 1960).
[35] A. Bohr and B. R. Mottelson, *Nuclear Structure* (W. A. Benjamin, Reading, MA, 1975), Vol. II.